

DC Circuit Breaker Evolution, Design, and Analysis

Mehdi Moradian ¹, Tek Tjing Lie ^{1,*} and Kosala Gunawardane ²

¹ Department of Electrical and Electronic Engineering, Auckland University of Technology, Auckland 1010, New Zealand; mehdi.moradian@autuni.ac.nz

² Department of Electrical Engineering, University of Technology Sydney, Ultimo 2007, Australia; kosala.gunawardane@uts.edu.au

* Correspondence: tek.lie@aut.ac.nz

Abstract: While traditional AC mechanical circuit breakers can protect AC circuits, many other DC power distribution technologies, such as DC microgrids (MGs), yield superior disruption performance, e.g., faster and more reliable switching speeds. However, novel DC circuit breaker (DCCB) designs are challenging due to the need to quickly break high currents within milliseconds, caused by the high fault current rise in DC grids compared to AC grids. In DC grids, the circuit breaker must not provide any current crossing and must absorb surges, since the arc is not naturally extinguished by the system. Additionally, the DC breaker must mitigate the magnetic energy stored in the system inductance and withstand residual overvoltages after current interruption. These challenges require a fundamentally different topology for DCCBs, which are typically made using solid-state semiconductor technology, metal oxide varistors (MOVs), and ultra-fast switches. This study aims to provide a comprehensive review of the development, design, and performance of DCCBs and an analysis of internal topology, the energy absorption path, and subcircuits in solid-state (SS)-based DCCBs. The research explores various novel designs that introduce different structures for an energy dissipation solution. The classification of these designs is based on the fundamental principles of surge mitigation and a detailed analysis of the techniques employed in DCCBs. In addition, our framework offers an advantageous reference point for the future evolution of SS circuit breakers in numerous developing power delivery systems.

Keywords: DC circuit breaker; mechanical DCCB; solid-state DCCB; hybrid DCCB; DC microgrids; DC circuit breaker topology; metal oxide varistor; surge absorption



Citation: Moradian, M.; Lie, T.T.; Gunawardane, K. DC Circuit Breaker Evolution, Design, and Analysis. *Energies* **2023**, *16*, 6130. <https://doi.org/10.3390/en16176130>

Academic Editor: Angela Russo

Received: 23 May 2023

Revised: 30 July 2023

Accepted: 18 August 2023

Published: 23 August 2023



Copyright: © 2023 by the authors. Licensee MDPI, Basel, Switzerland. This article is an open access article distributed under the terms and conditions of the Creative Commons Attribution (CC BY) license (<https://creativecommons.org/licenses/by/4.0/>).

1. Introduction

DC microgrids (MGs) are a modern form of electricity distribution system that use DC instead of AC to transmit and distribute electrical energy. In a DC MG, various distributed energy resources (DERs) such as photovoltaic (PV) systems, wind turbines, and energy storage devices are connected to a common DC bus through power electronics interfaces. DC MGs are becoming increasingly popular due to their numerous advantages over traditional AC grids, including improved energy efficiency, higher power quality, greater flexibility, and economical reasons in integrating renewable energy sources [1–3]. They are also considered to be an important solution for addressing the challenges of the increasing demand for electricity, energy security, and climate change mitigation.

However, the design and operation of DC MGs pose unique challenges, such as controlling power flow and maintaining stability and reliability, which require innovative solutions. As a result, research and development efforts in the field of DC MGs are ongoing, with the aim of improving their performance and expanding their application [4–6].

An overview of a typical DC MG is presented in Figure 1. DC circuit breakers are placed at various locations in the grid, near the renewable energy resources, transmission line, main grid, battery bank, and load sides to ensure microgrid protection and maintenance. The DC circuit breaker (CB) types vary due to the presence of different levels of

voltage and current paths within the network, ranging from generation to load. The primary objective of having a DCCB in DC systems is to protect the system against intentional or unintentional faults and voltage or current switching surges [7–10]. Table 1 provides a brief comparison between the DCCB specifications of some manufacturers [11–15]. The selection of DCCBs will be based on the working conditions, the voltage and current level, and the thermal capacity, which is substantially affected by I^2t of the beaker. The AC system can endure the fault current for a slightly longer period of time when it is experiencing a thermal overload or overcurrent, since the fault current rise rate is comparatively slow. Due to the DC system’s low short-circuit impedance and the rapid rising time of the fault current, it must be stopped immediately [16–18].

Furthermore, DCCBs are also utilized for maintaining the devices within the DC system. When a component of the system requires maintenance, the DCCB can safely interrupt the circuit, allowing the maintenance work to be carried out without posing a risk to personnel or damaging the equipment.

The DCCB system has enabled some researchers [19–21] to focus on DC MG fault current limiting, control, and clearing. These areas of study have been widened to include DC MG clusters.

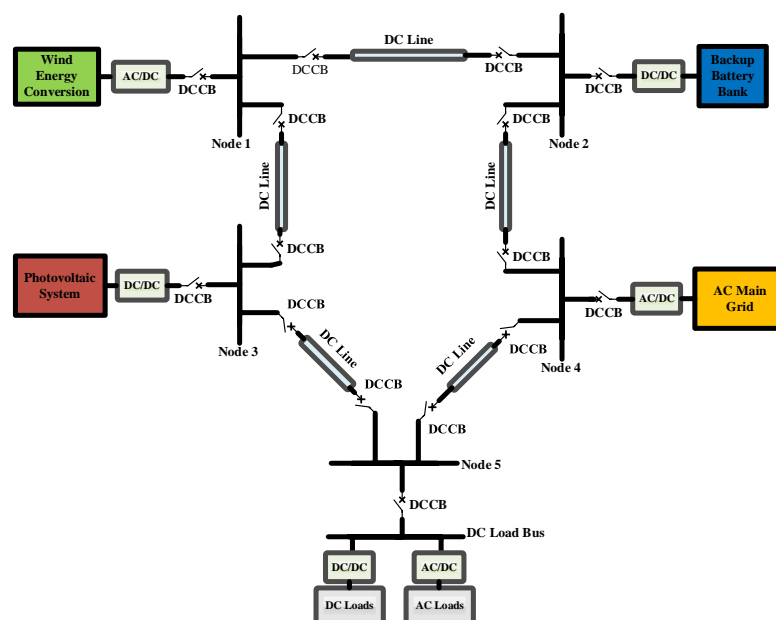


Figure 1. Overall topology of DC microgrids.

Table 1. Comparison of different types of commercialized DCCB’s applications.

Description	Schneider Electric	Eaton	Siemens	ABB	LS
Model	Power PacT JDC	CJGPVS, CKDPV	HDGD	SACE Emax	Susol
Rated current	30~1200 A	150~3000 A	50~1600 A	Up to 5000 A	16~1600 A
Performance voltage	500 VDC	600~1000 VDC	600 VDC	250~1000 VDC	500~1500 VDC
Breaking capacity	20 up to 50 KA	1.5 up to 42 KA	42 KA	65 KA	20 up to 50 KA
Ambient conditions	−10 to 60 °C	−40 to 70 °C	−25 to 70 °C	−40 to 70 °C	−25 to 55 °C
Operation time	≤30 ms	1 ms	70–300 ms	≤70 ms	≤40 ms

2. Surge Absorption Design Principle for DC Circuits

Surge voltages are voltage increases that usually occur for a duration from approximately one signal cycle to 1.5 s. These overshoots are typically triggered by the switching of high range loads and main grids. Although they are not as intense as sharp spikes, surges usually surpass the line voltage by around 20%, which can lead to the data corruption of computers, harm to devices, and inaccurate readings in supervision systems. If a surge

persists for more than two seconds, it is generally known as an overvoltage. Therefore, to protect a circuit against transients, it is necessary to restrict the voltage amplitude of the surge at each part of the circuit and deviate the current and voltage of the surge through protection-specific components to absorb the released energy. The likelihood of experiencing damage from a power surge is typically associated with the size of the sudden increase and the time span of the surge. Electric discharges and other transients in power systems exhibit rapid and intense properties in terms of both speed and magnitude (often several thousands of volts); hence, surge protection devices (SPDs) need to react promptly and manage considerable energy levels quickly to be effective. Typically, upstream circuit breakers or fuses cannot react quickly enough in response to the activation of the surge diverter because their reaction time is not as fast as the span of the transient impulse [22,23].

Essentially, all SPDs operate as voltage dividers [24]. Figure 2 demonstrates this concept with a series line impedance, Z_S , and a load impedance, Z_L . The source impedance, Z_S , is always present due to the impedance of the system wiring and transient source. Since Z_L is significantly larger than Z_S , a greater voltage is generated across the load, which leads to detrimental consequences. When an impedance-blocking device like a metal oxide varistor (MOV_{block}) is linked in series, as depicted in Figure 2a, its impedance rises in response to the surge's frequency component dependents. This causes a decrease in the load voltage. Thus, this type of series SPD topology is not conventional. When a shunt SPD element, such as MOV_{shunt} with an impedance of Z_{MOV} as shown in Figure 2b, is used, its impedance decreases during high-voltage surges, allowing a shunt current to flow through it and absorb the surge energy. If possible, components of Z_S should be selected to increase its value and mitigate the surge, thereby reducing the stress on the bypass device.

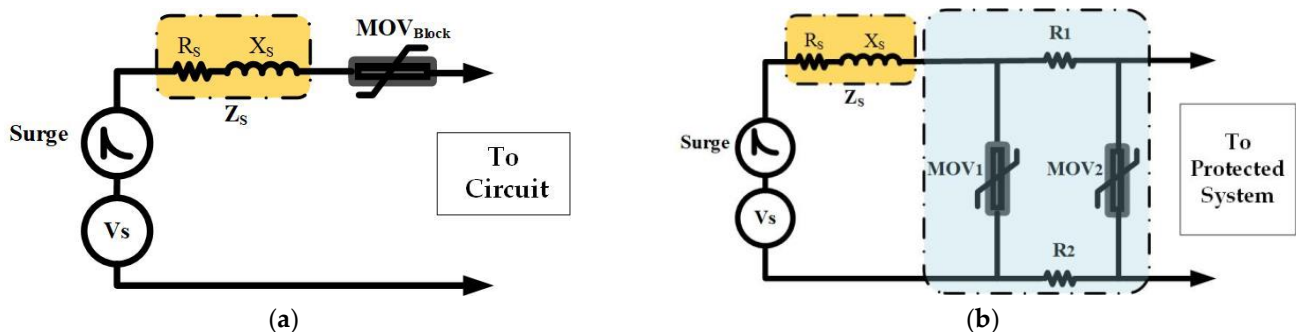


Figure 2. Voltage division methodology in transient surge protector design: (a) with a blocking device in the series configuration; (b) With a shunting device configuration.

An optimal SPD should minimize the transmitted surge energy to the load to protect both the load and the SPD against any hazard. This transmitted energy can be determined by integrating the surge voltage and current over time, represented as $\int v i dt$. An effective SPD should achieve a lower voltage across the load (known as clamping voltage) to restrict the current flowing through the load. It should also possess characteristics such as low dynamic resistance and quick response time. Additionally, extra factors such as longevity, repeatability, board size, cost, reliability, and a fail-safe mechanism are crucial considerations in the design of an SPD.

In DC calculations, given zero frequency ($f = 0$), impedance is considered as pure resistance. However, in case of a high frequency surge occurrence, impedance behavior changes by created inherent inductance. Surge frequency for a $20 \mu s$ length time is 50 kHz; for $50 \mu s$, it is 20 kHz. Thus, the impedance amount of the circuit ($Z = R + jX$) should be calculated whether the inductance is negligible or not.

Since shunt structures are more suitable for SPD designs, the dissipated energy in a MOV can be computed using the following method for the estimation of voltage, V_{MOV} , and current, I_{MOV} , of the MOV as expressed in Equations (1) and (2):

$$V_{MOV} = \frac{Z_{MOV}}{Z_{MOV} + Z_S} \times V_{Surge} \quad (1)$$

$$I_{MOV} = \frac{Z_L}{Z_L + Z_{MOV}} \times i_{Surge} \quad (2)$$

Therefore, the energy that is dissipated across the MOV, E_{MOV} , during the surge time denoted as t_{surge} can be expressed in Equation (3) as follows:

$$E_{MOV} = V_{MOV} I_{MOV} t_{surge} = \frac{Z_{MOV} Z_L}{(Z_{MOV} + Z_S)(Z_L + Z_{MOV})} V_{Surge} i_{Surge} t_{surge} \quad (3)$$

The above calculation could assist designers in choosing the appropriate components for their SPD design.

A typical practical protector design with nonlinear devices such as MOVs and bidirectional breakover devices (BBDs) for a three-wire DC system is illustrated in Figure 3. Capacitors represent additional near short-circuit paths to the surges and offer exceptional protection as well. If the maximum induced voltage is greater than the corresponding MOV's firing voltage, the MOV will activate and conduct a high current immediately. This causes a clamping voltage to form across the MOV terminals, and it absorbs the released energy over the surge duration. This protects the critical load from the surge voltage danger. Additionally, the surge energy is further filtered by the LC filters on the path. The series inductor's $L\omega$ impedance and the parallel capacitor's $\frac{1}{C\omega}$ impedance absorb more energy of the HV transient. If there is any residual HV transient, the BBDs at the end of the protection path will absorb it by firing, provided that the peak of the remaining surge surpasses the BBD's trigger voltage [25].

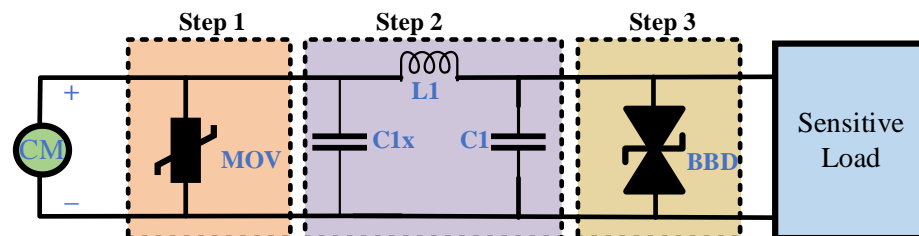


Figure 3. Practical surge protector topology against common mode (CM) surge for a three-wire DC system.

The total dissipated energy (E_D) in the system will be determined as the sum of the dissipated energy during the three steps of surge protection, as expressed in Equation (4).

$$E_D = E_{step1} + E_{step2} + E_{step3} \quad (4)$$

$$V_{MOV} = \frac{Z_{MOV}}{Z_S + Z_{MOV}} V_{Surge} \quad (5)$$

$$V_{C1} = \frac{Z_{C1}}{Z_{C1} + Z_{L1}} V_{MOV} \quad (6)$$

$$V_{SL} = V_{BBD} = V_{C1} = \frac{Z_{MOV} \times Z_{C1}}{(Z_S + Z_{MOV}) \times (Z_{C1} + Z_{L1})} \times V_{Surge} \quad (7)$$

$$i_{surge} = i_{MOV} + i_{C1x} + i_{L1} \quad (8)$$

$$i_{L1} = i_{C1} + i_{BBD} + i_{SL} \quad (9)$$

$$i_{MOV} = \frac{Z_s}{Z_s + Z_{MOV}} i_{surge} \quad (10)$$

$$i_{C1x} = \frac{Z_s}{Z_s + Z_{C1x}} i_{surge} \quad (11)$$

$$i_{C1} = \frac{Z_{L1}}{Z_{L1} + Z_{C1}} i_{L1} \quad (12)$$

$$i_{BBD} = \frac{Z_{L1}}{Z_{L1} + Z_{BBD}} i_{L1} \quad (13)$$

$$i_{L1} = \frac{(Z_{L1} + Z_{C1})(Z_{L1} + Z_{BBD})}{Z_{BBD}Z_{C1} - Z_{L1}^2} \times i_{SL} \quad (14)$$

$$i_{L1} = Xi_{SL} \quad (15)$$

Given the component impedances and a constant value, X, the surge current can be calculated using Equation (14), which can then be used to determine the sensitive load current (Equation (16)):

$$i_{SL} = Y \times i_{surge} \quad (16)$$

$$Y = \frac{Z_{BBD}Z_{C1} - Z_{L1}^2}{(Z_{L1} + Z_{C1})(Z_{L1} + Z_{BBD})} \times \frac{Z_{MOV}Z_{C1x} - Z_s^2 - Z_sZ_{C1x}}{(Z_s + Z_{MOV})(Z_s + Z_{C1x})} \quad (17)$$

Therefore, the amount of dissipated energy in each component in the circuit can be determined separately by considering the provided estimated values of the voltage and current of each component multiplied by the time, as shown, e.g., in Equation (3).

3. DC Circuit Breaker Topologies

There are three fundamental topologies of DC circuit breakers [26–28]. Other researchers have developed these designs, but electromechanically based circuit breakers are no longer used in DC topology system designs due to the significant disadvantage of their low-speed performance. The three topologies are as follows:

1. mechanical (resonance) DC circuit breakers (M-DCCB);
2. solid-state (static) DC circuit breakers (SS-DCCB);
3. hybrid DC circuit breakers (H-DCCB).

In the subsequent stage, there will be an examination and thorough discourse on the structure and efficiency of various topologies.

The objective of Figure 4 is to demonstrate the significant contrast in both reaction time and current-limiting capacity between the different topologies of DCCBs. Since the control of semiconductor devices as active components is governed by a comparatively low-power external signal, the activation of the SS-DCCB turn-off and current-limiting mechanism can take place in a matter of microseconds.

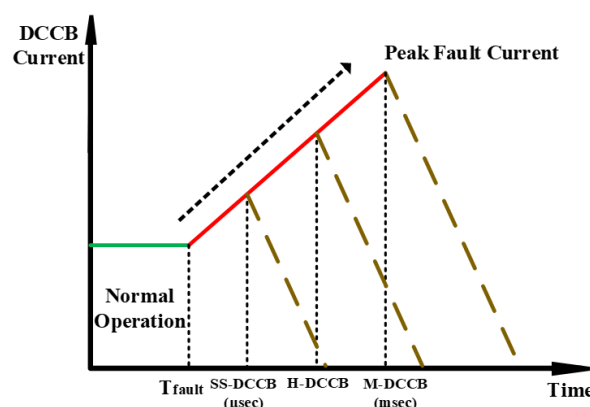


Figure 4. Response time comparison between DCCBs in fault absorption.

Efforts to develop DCCBs that utilize resonance began in the 1980s. Topology 1 (M-DCCB) in Table 2 provides an overview of the topology, which involves mechanical switches that interrupt the current when a zero crossing is created through an LC path (known as a forced current diverted commutation line) that runs in parallel with the main electromechanical breaker. The topology also comprises an energy absorption branch, which consists of MOVs. Although newer topologies mentioned in this section may have advantages over the resonance topology, such as lower resistive on-state loss, it may still have practical applications for load switching. The resonance DC breaker topology is comprised of three primary branches [27]:

1. the normal current flow line;
2. the forced current diverted commutation line;
3. the surge mitigation subcircuit.

During a typical operation, the current follows the intended line. However, if the breaker is instructed to interrupt the current, a mechanical switch will open, resulting in an arc and a change in the current direction into a different path. This change generates current oscillations. The arc causes a voltage drop that contributes to these oscillations, which in turn help to extinguish the arc by crossing the zero current point. Afterwards, the current flows into an absorption subcircuit to dissipate any remaining induced energy of the system.

The internal structure of the electrical contact in a molded case circuit breaker (MCCB) double break operating mechanism is presented in Table 2 (see Topology 1). The double-breaking contact system is a highly advanced design for low voltage circuit breaker contacts and was patented by Siemens in 2007. The U-shaped contact points help to reduce the intensity of the shock caused by a surge in the breaker by producing a magnetic field that rotates 180 degrees in the opposite direction. This design simplifies the disconnection of the double-breaking mechanism [29,35].

To improve and supply the quick interruption during the fault or surges in DC systems, SS-DCCBs have been used. The solid-state topology employs semiconductor devices such as IGBTs, MOSFETs, GTOs, and Thyristors in conjunction with a MOV and/or a capacitor to interrupt the flow of the electrical current. During regular operation, the current flows through the semiconductor devices. To halt the current, the devices are deactivated, and the current is rerouted into the paralleled subcircuit, which acts as both the commutation and energy-absorbing path. The MOVs discharge the energy accumulated in the system, much like in the resonance topology. The SS-DCCB topology illustrates a solid-state-based configuration that employs IGBTs and diodes for bi-directional applications. The figure demonstrates a solid-state DC breaker for unidirectional configuration. The topology of bi-directional current interruptions could be achieved by positioning an IGBT of the same range in anti-series with an anti-parallel diode. More breaker cells can be added in series to raise the rated voltage level [36]. Even though the SSCB can break the current swiftly enough for fault current disruption, the semiconductors conduct the current during

typical working conditions, causing high losses due to the voltage drop over the breaker, particularly in high voltage applications [31,37].

Table 2. Fundamental topologies of DCCBs.

<p>Topology 1, M-DCCB [16,29]</p>			<p>Advantage: High breaking capacity Disadvantage: Low speed Large size Significant arc production</p>
<p>Topology 2, SS-DCCB [30,31]</p>			<p>Advantage: Very fast Small size Low loss Disadvantage: Low capacity</p>
<p>Topology 3, H-DCCB [28,32–34]</p>		<p>Advantage: High breaking capacity Fast Disadvantage: Expensive</p>	

A typical SSCB comprises several crucial elements, including power semiconductor devices, gate drivers, cooling mechanisms, voltage clamping circuits, fault detection systems, sense and trip electronics, and an auxiliary power supply. In Table 2, the theoretical performance of a standard SSCB is depicted. The number of power semiconductors needed will vary depending on the application’s voltage and current ratings, the power semiconductor technology, and the breaker’s topology. Even though gate drivers with an auxiliary power supply are already on the market, several researchers are investigating ways to enhance the gate driver’s capabilities to create high-performance SSCBs and integrate multiple functions into a single unit [31].

Hybrid topologies combine both mechanical switches and semiconductor devices. Recent research papers suggest that ABB and ALSTOM have created DC circuit breaker

prototypes using this approach, and they show potential as promising technologies. The H-DCCB topology provides an overview of the hybrid DC circuit breaker, which can be viewed as an extension of an IGBT-based solid-state topology. The utilization of thyristors in the design enables this topology to be appropriate for HVDC circuit breaker designs, as it can handle large voltage and current levels effectively [38–43]. The breaker includes an additional branch with a mechanical low resistance ultra-fast disconnecter (UFD) and a load commutation switch (LCS). The LCS, like the solid-state DC breaker, is designed to interrupt current flow, but it has a limited number of breaker cells that can only transfer the current to the main breaker. To address the issue of conduction losses in the solid-state topology, the hybrid topology allows for the nominal current to flow through the LCS and a UFD under regular operation. When an interruption command is received, the LCS, like the solid-state breaker, turns off and transfers the current to the main breaker. Following the commutation, the UFD opens to isolate and protect the LCS from voltage drops caused by the main breaker's interruption of the current. The UFD is a crucial element in minimizing losses during regular operations and achieving rapid current interruption. It operates as an electromagnetic actuator, utilizing magnetic forces to achieve the fast-switching speed necessary for efficient circuit protection. According to ABB, their DC circuit breaker can eliminate faults within 5 ms. The role of the current limiting reactor is to restrict the high slope of the fault current. In addition, a switch that operates in parallel with the hybrid DC breaker is also present to provide physical isolation following the clearance of the fault current. To determine the current and energy dissipation in these circuit breakers during a fault, certain circuit parameters must be considered. Following a circuit fault in a DC system, most of the fault current redirected through the H-DCCB is attributable to the IGBTs within the breaker [44–46]. The fault current can be denoted in Equation (18), as follows:

$$i_f = I_{line} + \frac{V_{IGBT}}{L_{line} + L_{CLR}} \times (t - t_1) \quad (18)$$

where I_{line} is the pre-fault current, L_{CLR} is the current limiting reactor inductance, and t_1 is the fault time. The current of the IGBT switch will be calculated using Equation (19):

$$i_{IGBT} = I_{line} + \frac{V_{IGBT}}{L_{line} + L_{CLR}} \times t_2 \quad (19)$$

where t_2 is the performance time of the IGBT switch.

To calculate the dissipated energy of the MOV, the voltage at the protection level during t_3 (MOV performance time) is assumed to remain constant. The maximum amount of energy dissipated by the MOV in each series part is then determined by Equation (20):

$$E_{MOV} = \left[I_{line} + \frac{V_{IGBT}}{L_{line} + L_{CLR}} \times t_2 \right] \times V_{MOV} \times \frac{t_3}{2} \quad (20)$$

Thus, the dissipated energy between each individual series cell in H-DCCB could be calculated separately by the presented formula [47,48].

4. Design Improvements of DCCBs for DC Microgrid Application

The upcoming section will examine three novel and distinct classifications of the DCCB's energy absorption techniques:

- 4.1. MOV-based DCCBs;
- 4.2. capacitor-based DCCBs;
- 4.3. hybrid MOV–Cap DCCBs.

The most crucial section in DCCBs for absorption of the released energy during switching and faults is the energy absorption part. In this section, we compared a wide range of studies that suggested several designs to redirect the surge through solid-state components to technically absorb the released energy. The constructed DCCB worked admirably in each of the approaches that were discussed, and the outcomes are pleasing.

The difference is between their technology, the performance voltage and current level, and the response time, which is a key factor in DCCB designs.

4.1. MOV-Based DCCBs

For DCCBs based on MOVs, the circuit breaker’s embedded MOV completely handles surge absorption. Different designs define the strategy for absorbing the released energy [49–52].

The significant drawback of these designs is that the MOVs deteriorate over time when exposed to surges [22,30].

The separated MOV technique shown in Table 3 illustrates an approach that involves two distinct MOVs placed in specific locations within a circuit, to isolate the two functions of the MOV, namely voltage clamping and energy absorption. This proposed approach aims to separate the two functions of MOVs, allowing them to operate independently and more efficiently. The result shows successful test and surge absorption through the paralleled MOV’s circuit. However, the test is restricted to a small range of voltage and current amplitudes.

Table 3. A comparative study of three conventional MOV-based DCCB designs.

Description	Topology 1 [53]	Topology 2 [54]	Topology 3 [55]
Proposed Model			
Model Verification			
Technique	Separated MOV	Ground Clamping	MC FCL
Technology	MOV-IGBT	MOV-MOSFET, IGBT	MOV-IGBT
V _{dc} /I _{dc}	30 v/2.5 A	400 v/4 A	500 v/380 A
Response Time	0.4 μs	50 ms	1.8 ms
Number of Passive Components	4	6	8
Number of Active Components	1	2	≥4

The ground clamping strategy illustrates a new DCCB design that uses a current limiter to absorb the surge voltage [54]. This SSCB design consists of several components including a main switch (S₂) that conducts the line current and prevents source voltage before and after breaker operation. Additionally, the design includes a MOV to demagnetize the energy stored in the system inductor, a ground clamping switch (S₁) that bypasses the DC bus, and a current-limiting inductor (L₂) with its resistive energy absorber. In this design, minimum current limiting inductance could be determined by Equation (21) according to

the bus voltage, V_{DC} , the breaking time, T_{Break} , the zero current detection time, T_{det} , the saturation current of the inductor, I_{Lsat} , and the threshold current of I_0 :

$$L_s > \frac{V_{DC}(T_{Break} + T_{det})}{I_{Lsat} - I_0} \tag{21}$$

Furthermore, the magnetic coupling fault current limiter (MC FCL) technique proposes a fault current limiting design with a magnetic coupling auxiliary circuit in the input of the circuit breaker to limit the severity of the current shocks. In this study, the released energy is coordinated to be dissipated in both the MOV and the resistance in the secondary of the transformer.

Overall, while various techniques for surge absorption have been successful in damping surges and fault currents, there are design issues that need to be addressed. For example, many designs rely on metal oxide varistors (MOVs) for surge absorption, but often fail to consider their limitations, as their ability to damp surges can weaken, and they will degrade over time.

4.2. Capacitor-Based DCCBs

To enhance the design of DCCBs, some studies have explored the use of capacitor-based technology for both commutating and surge absorption purposes. This approach involves a bridge-type capacitor-commutation unit that serves to buffer the device voltage and is considered an independent method for improving DCCB design [56,57]. Table 4 provides a concise overview of the recent designs, highlighting their points of comparison.

Table 4. A comparative study of three conventional capacitor-based DCCB designs.

Description	Topology 1 [58]	Topology 2 [59]	Topology 3 [60]
Proposed Model			
Model Verification			
Technique	A/C Circuit	VI- PMA	Soft-switched
Technology	Cap-IGBT	Cap-IGBT	Cap-MOSFET
V_{dc}/I_{dc}	283 v/43.5 A	750 v/300 A	240 v/50 A
Response Time	15 ms	9.6 ms	20 ms
Number of Passive Components	2	7	12
Number of Active Components	3	5	5

All three capacitor-based DCCB designs mentioned in Table 4 redirect surges to a subcircuit to reduce the impact of energy released during DC system faults or surges. They effectively absorb energy using specific techniques. However, the designs differ in terms of their response time, their voltage and current levels, and the components used in the circuit.

Other studies have employed unidirectional and bidirectional Z-source DCCB (Z-s DCCB) designs, whose strategy is focused on a capacitor-based design [61–66]. Z-s DCCBs show potential as suitable options for protect low- and medium-voltage distribution networks, along with DC equipment, among the various configurations available, because of their uncomplicated structure, control mechanism, and economical price [67]. Figure 5 shows the general layout of bidirectional Z-s DCCBs, where two sets of isolated thyristors are arranged in parallel to facilitate the flow of the current in both directions.

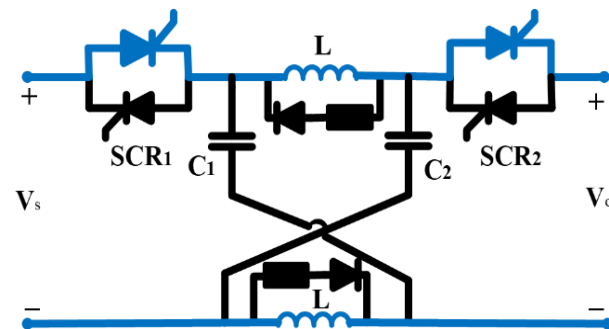


Figure 5. A bidirectional Z-s DCCB [67].

In these designs, electrolytic capacitors for surge absorption are utilized, but these components have limited capacity and cannot dissipate the energy released by high-voltage faults with a longer duration and have a limited lifespan due to their chemical structure.

4.3. Hybrid MOV–Cap DCCBs

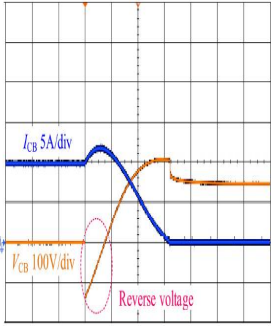
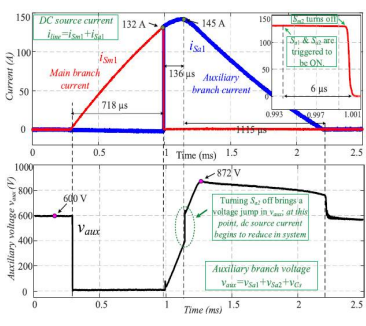
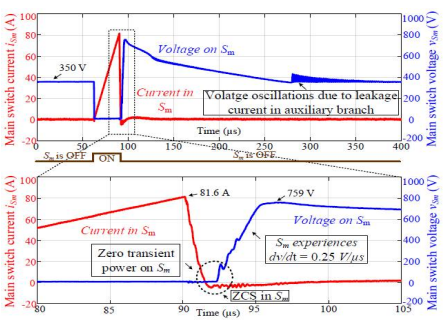
Several studies have proposed novel designs of hybrid MOV–Cap DCCBs to overcome the weakness of MOV degradation and the restricted capability of capacitors to absorb energy [68–71].

All designs shown in Table 5 effectively perform fast through different techniques. The capacitor discharge path is considered for all models, and the voltage and current levels in the circuits are different.

Table 5. A comparative study of three conventional hybrid MOV–Cap DCCB designs.

Description	Topology 1 [72,73]	Topology 2 [74]	Topology 3 [75]
Proposed Model			

Table 5. Cont.

Description	Topology 1 [72,73]	Topology 2 [74]	Topology 3 [75]
Model Verification			
Technique	AT CB-DCCB	TIM-Pack	LCC-AIC
Technology	MOV-Cap Thyristor	MOV-Cap Thyristor-IGBT	MOV-Cap SiC MOSFET
V_{dc}/I_{dc}	150 v/10 A	600 v/145 A	350 v/90 A
Response Time	1.6 ms	6 μ s	4 μ s
Number of Passive Components	5	5	9
Number of Active Components	4	4	2

In the active thyristor CB (AT-CB) technique, a bidirectional, low-loss DCCB with a reliable opening process based on a simple hybrid design for a capacitor and a MOV is implemented. This technique is more suitable for medium-voltage DC systems [72].

$$t_q = \frac{C_b V_n}{\alpha I_{fmax}} \quad (22)$$

$$C_b = \frac{\alpha t_q I_{fmax}}{V_n} \quad (23)$$

Therefore, the value of the bypass capacitor can be approximated using Equation (23), which involves determining the recovery time, t_q , which can be calculated using Equation (22), where the values for the maximum allowable fault, I_{fmax} , and the desired coefficient, α , are inserted.

Other techniques involving active injection circuits (LCC-AICs) based on TIM-Pack (Thyristor-IGBT-MOV) and on an inductor capacitor-capacitor, shown in Table 5, switch fault currents into the designed subcircuits within a couple of microseconds to improve reliability.

5. Design Improvements

Various surge absorption techniques for designing DCCBs in nominal voltage ranges that span from a few hundred volts to tens of kV have been discussed in the literature. The power rate, voltage, and flowing current level in a DC microgrid are directly linked to the semiconductor device utilized in its design. As a result, the design and techniques employed should be adapted for varying levels of power in the microgrid. In the circuit design of DCCBs, the number of passive and active components used plays a crucial role in determining the most cost-effective topologies in terms of the rate of DC system power. It is also important to consider the lifespan of the circuit components by assessing the weaknesses of each part during the design process. Regarding the reliability of the

circuit, there is a lack of detailed comparison in the literature, specifically in terms of the vulnerabilities of the components such as deterioration, chemical-based materials, and limited energy capacity.

This paper focuses on proposing new ideas for improving the design of the surge absorption subcircuit in the evolution of DCCB designs. Table 3 focuses on the performance of the circuit and the task of energy absorption, which currently relies on MOV-based subcircuits. However, the weakness in protection performance as well as MOV degradation are not taken into consideration. A MOV alone is unable to protect a circuit against short circuits and overcurrent situations. Therefore, when designing a DCCB for DC protection with an MOV energy absorber, it is crucial to consider current limitations. This aspect is addressed in the designs utilizing a ground clamping strategy and MC FCL techniques.

Hybrid designs are typically employed to address the performance limitations of previous designs and enhance their features. A hybrid design in the energy absorber can mitigate the degradability, overcurrent, and short circuit protection issues associated with MOVs in Table 3, as well as the low capacity and chemical-based weaknesses of capacitors in Table 4. In a hybrid design, the tension in the circuit is divided among various shock absorber components, effectively covering these weaknesses. This concept is most evident in the designs proposed by TIM-Pack and LCC-AIC techniques.

6. Prospective Future Advancement

Here are a few possible advancements that can be pursued in the future:

- The surge absorption techniques and subcircuits in DCCB design can be studied to cover the existing limitations.
- The DCCB designs can be integrated in terms of performance and a higher breaking capacity against the faults and switching of DC circuits.
- The reliability and lifetime of DCCBs can be improved by using non-chemical, non-degradable components for surge, fault, and switching effect absorption.
- Costs can be reduced by substituting a minimal amount of degradable components, and alternative components, such as resistance, can be used instead of expensive ones, such as MOVs.
- Power loss can be minimized through design improvements, which could involve reducing both switching power loss resulting from semiconductor switching and passive component loss from elements such as current limiters and snubber resistors during regular system operations. This can lead to a more efficient performance with reduced power dissipation.

7. Conclusions

A DCCB, as a significant part of the DC MG topology, protects and improves the reliability of modern power systems. In this article, the surge absorption principle in DC systems was reviewed to illustrate the process of limiting voltage and current transients that occur in DC systems due to switching operations or lightning strikes. Furthermore, three-level SPD design estimations for sensitive load were determined, and they ensure that sensitive loads are protected from transients.

Three main topologies of the DCCB design evolution, including the M-DCCB, SS-DCCB, and H-DCCB topologies, were investigated and reviewed. Each topology has its advantages and disadvantages, and the choice of topology depends on the specific application requirements. Particularly, the energy absorption subcircuits of DCCBs were studied, which were separated into three sub-designs: MOV-based, capacitor-based, and hybrid MOV-Cap-based designs. Various techniques were then examined and discussed to identify the optimal design approach for different applications. Finally, design improvement factors and the future development of DCCBs were discussed. These include the use of advanced materials, such as wide-bandgap semiconductors, and the integration of DCCBs with other protection devices to improve overall system reliability.

The surge absorption technique and design plays a critical role in ensuring the reliable performance of DC MGs and DCCBs. The protection of modern power systems primarily depends on the techniques employed in DCCBs. Enhancing the subcircuit design responsible for energy absorption and considering design improvement factors will contribute to the advancement of DCCBs in the context of future power systems.

Author Contributions: Conceptualization, methodology, writing—original draft preparation, M.M.; writing—review and editing, supervision, investigation, and visualization, T.T.L. and K.G. All authors have read and agreed to the published version of the manuscript.

Funding: This research received no external funding.

Data Availability Statement: No additional source data are required.

Acknowledgments: The authors would like to acknowledge MBIE SSIF AETP project entitled ‘Architecture of the Future Low-Carbon, Resilient, Electrical Power System’ for the financial support.

Conflicts of Interest: The authors declare no conflict of interest.

References

1. Rezk, H.; Ghoniem, R.M.; Ferahtia, S.; Fathy, A.; Ghoniem, M.M.; Alkanhel, R. A Comparison of Different Renewable-Based DC Microgrid Energy Management Strategies for Commercial Buildings Applications. *Sustainability* **2022**, *14*, 16656. [CrossRef]
2. Lotfi, H.; Khodaei, A. Hybrid AC/DC microgrid planning. *Energy* **2017**, *118*, 37–46. [CrossRef]
3. Papari, B.; Edrington, C.S.; Bhattacharya, I.; Radman, G. Effective Energy Management of Hybrid AC–DC Microgrids with Storage Devices. *IEEE Trans. Smart Grid* **2019**, *10*, 193–203. [CrossRef]
4. Vuyyuru, U.; Maiti, S.; Chakraborty, C. Active Power Flow Control Between DC Microgrids. *IEEE Trans. Smart Grid* **2019**, *10*, 5712–5723. [CrossRef]
5. Jain, D.; Saxena, D. Comprehensive review on control schemes and stability investigation of hybrid AC-DC microgrid. *Electr. Power Syst. Res.* **2023**, *218*, 109182. [CrossRef]
6. Baidya, S.; Nandi, C. A comprehensive review on DC Microgrid protection schemes. *Electr. Power Syst. Res.* **2022**, *210*, 108051. [CrossRef]
7. Montoya, R.; Poudel, B.P.; Bidram, A.; Reno, M.J. DC microgrid fault detection using multiresolution analysis of traveling waves. *Electr. Power Energy Syst.* **2022**, *135*, 107590. [CrossRef]
8. Bayati, N.; Balouji, E.; Baghaee, H.R.; Hajizadeh, A.; Soltani, M.; Lin, Z.; Savaghebi, M. Locating high-impedance faults in DC microgrid clusters using support vector machines. *Appl. Energy* **2022**, *308*, 118338. [CrossRef]
9. Ibrahim, M.H.; Badran, E.A.; Abdel-Rahman, M.H. On the DC Microgrids Protection Challenges, Schemes, and Devices—A Review. In *DC Microgrids: Advances, Challenges, and Applications*; Wiley: Hoboken, NJ, USA, 2022. [CrossRef]
10. Zhang, Q.; Hu, W.; Liu, Y.; Zhang, H.; Wang, H. A novel smooth switching control strategy for multiple photovoltaic converters in DC microgrids. *J. Power Electron.* **2022**, *22*, 163–175. [CrossRef]
11. Available online: <https://new.abb.com/low-voltage/products/circuit-breakers> (accessed on 27 March 2023).
12. Available online: <https://www.se.com/ww/en/product-range/44215156-compact-for-dc-networks-new-generation> (accessed on 27 March 2023).
13. Available online: <https://www.eaton.com/nz/en-gb/products/electrical-circuit-protection/circuit-breakers.html> (accessed on 27 March 2023).
14. Available online: <https://www.siemens.com/global/en/products/energy/low-voltage/components/sentron-protection-devices.html> (accessed on 27 March 2023).
15. Available online: https://www.ls-electric.com/products/category/Smart_Power_Solution/DC_Component (accessed on 27 March 2023).
16. Huo, Q.; Xiong, J.; Zhang, N.; Guo, X.; Wu, L.; Wei, T. Review of DC circuit breaker application. *Electr. Power Syst. Res.* **2022**, *209*, 107946. [CrossRef]
17. Corzine, K.A. Circuit Breaker for DC Micro Grids. In Proceedings of the IEEE First International Conference on DC Microgrids (ICDCM), Atlanta, GA, USA, 7–10 June 2015. [CrossRef]
18. Maqsood, A.; Corzine, K.A. DC Microgrid Protection: Using the Coupled-Inductor Solid-State Circuit Breaker. *IEEE Electr. Mag.* **2016**, *4*, 58–64. [CrossRef]
19. Bayati, N.; Baghaee, H.R.; Savaghebi, M.; Hajizadeh, A.; Soltani, M.N.; Lin, Z. DC Fault Current Analyzing, Limiting, and Clearing in DC Microgrid Clusters. *Energies* **2021**, *14*, 6337. [CrossRef]
20. Srivastana, C.; Tripathy, M. DC microgrid protection issues and schemes: A critical review. *Renew. Sustain. Energy Rev.* **2021**, *115*, 111546. [CrossRef]
21. Beheshtaein, S.; Cuzner, R.M.; Forouzesh, M.; Savaghebi, M.; Guerrero, J.M. DC microgrid protection: A comprehensive review. *IEEE J. Emerg. Sel. Top. Power Electron.* **2019**, *12*. [CrossRef]

22. Kularatna, N.; Ross, A.S.; Fernando, J.; James, S. *Design of Transient Protection Systems-Including Supercapacitor Based Design Approaches for Surge Protectors*; Elsevier: Amsterdam, The Netherlands, 2019; ISBN 978-0-12-811664-7.
23. Salman, S.; Xin, A.; Masood, A.; Iqbal, S.; Hanan, M.; Jan, M.U.; Khan, S. Design and Implementation of Surge Protective Device for Solar Panels. In Proceedings of the 2018 2nd IEEE Conference on Energy Internet and Energy System Integration (EI2), Beijing, China, 20–22 October 2018. [CrossRef]
24. Ceballos, C.R.; Chejne, F.; Perez, E.; Osorio, A.; Correa, A. Study of the behavior of low voltage ZnO varistors against very fast transient overvoltages (VFTO). *Electr. Power Syst. Res.* **2023**, *214*, 108937. [CrossRef]
25. Kularanta, N.; Gunawardane, K. *Energy Storage Devices for Renewable Energy-Based Systems—Rechargeable Batteries and Supercapacitors*, 2nd ed.; Academic Press: Cambridge, MA, USA; Elsevier: Amsterdam, The Netherlands, 2021; ISBN 978-0-12-820778-9.
26. Zheng, S.; Kheirollahi, R.; Pan, J.; Xue, L.; Wang, J.; Lu, F. DC Circuit Breakers: A Technology Development Status Survey. *IEEE Trans. Smart Grid* **2022**, *13*, 3915–3928. [CrossRef]
27. Norum, E.Ø. Design and Operation Principles of DC Circuit Breakers-Development of a Solid-State DC Breaker for the NTNU/SINTEF Smart Grid and Renewable Energy Laboratory. Master's Thesis, Norwegian University of Science and Technology, Trondheim, Norway, 2016.
28. ABB Inc. Handbook. ABB Circuit Breakers for Direct Current Applications. 2010. 888-385-1221. Available online: <https://www.abb.us/lowvoltage,1SXU210206G0201> (accessed on 9 March 2023).
29. Ferree, J. Double-Breaking Contact System for a Low Voltage Circuit Breaker, a Molded Case Circuit Breaker Comprising the Double-Breaking Contact System, and a Method for Breaking a Circuit. US Patent US8159139B2, 17 April 2012.
30. Ravi, L.; Zhang, D.; Qin, D.; Zhang, Z.; Xu, Y.; Dong, D. Electronic MOV-Based Voltage Clamping Circuit for DC Solid-State Circuit Breaker Applications. *IEEE Trans. Power Electron.* **2022**, *37*, 7561–7565. [CrossRef]
31. Rodrigues, R.; Du, Y.; Antoniazzi, A.; Cairoli, P. A review of solid-state circuit breakers. *IEEE Trans. Power Electron.* **2021**, *36*, 364–377. [CrossRef]
32. Tu, Y.; Pei, X.; Zhou, W.; Li, P.; Wei, X.; Tang, G. An integrated multi-port hybrid DC circuit breaker for VSC-based DC grids. *Electr. Power Energy Syst.* **2022**, *142*, 108379. [CrossRef]
33. He, J.; Lyu, H.; Li, B.; Li, Y.; Wen, W.; Spier, D.W.; Araujo, E.P.; G.-Bellmunt, O. A Passive Thyristor-Based Hybrid DC Circuit Breaker. *IEEE Trans. Power Electron.* **2023**, *38*, 1791–1805. [CrossRef]
34. Augustin, T.; Becerra, M.; Nee, H.P. Enhanced Active Resonant DC Circuit Breakers Based on Discharge Closing Switches. *IEEE Trans. Power Deliv.* **2021**, *36*, 1735–1743. [CrossRef]
35. Shea, J.J. Low Voltage Power Distribution Level DC Circuit Breaking. In Proceedings of the 4th International Conference on Electric Power Equipment—Switching Technology (ICEPE-ST), Xi'an, China, 22–25 October 2017. [CrossRef]
36. Ludin, G.A.; Amin, M.A.; Matayoshi, H.; Rangarajan, S.S.; Hemeida, A.M.; Takahashi, H.; Senjyu, T. Solid-State DC Circuit Breakers and Their Comparison in Modular Multilevel Converter Based-HVDC Transmission System. *Electronics* **2021**, *10*, 1024. [CrossRef]
37. Zhu, J.; Zeng, Q.; Yang, X.; Zhou, M.; Wei, T. A Bidirectional MVDC Solid-State Circuit Breaker Based on Mixture Device. *IEEE Trans. Power Electron.* **2022**, *37*, 11486–11490. [CrossRef]
38. Zhang, X.; Zhuo, C.; Yang, X. A natural commutation current topology of hybrid HVDC circuit breaker integrated with limiting fault current. *IET Gen. Trans. Dist.* **2023**, *17*, 1509–1524. [CrossRef]
39. Yu, A.P.; Guo, B.X.; Wang, C.L.; Zhou, D.Z.; Wang, E.G.; Zhang, F.Z. Lifetime estimation for hybrid HVDC breakers. *Electr. Power Energy Syst.* **2020**, *120*, 106035. [CrossRef]
40. Heidary, A.; Bigdeli, M.; Rouzbehi, K. Controllable reactor based hybrid HVDC breaker. *High Voltage* **2020**, *5*, 543–548. [CrossRef]
41. Xu, X.; Chen, W.; Liu, C.; Sun, R.; Li, Z.; Zhang, B. An Efficient and Reliable Solid-State Circuit Breaker Based on Mixture Device. *IEEE Trans. Power Electron.* **2021**, *36*, 9767–9771. [CrossRef]
42. Liu, Y.; Li, B.; Yin, L.; Zheng, J.; Duan, Z.; Li, Z. Hybrid DC circuit breaker with current-limiting capability. *J. Power Electron.* **2022**, *23*, 700–711. [CrossRef]
43. Zhang, S.; Zou, G.; Wei, X.; Zhou, C.; Zhang, C. Multiport Current-Limiting Hybrid DC Circuit Breaker for MTdc Grids. *IEEE Trans. Ind. Electron.* **2023**, *70*, 4727–4738. [CrossRef]
44. Liu, Y.; Xia, T.; Li, D. Hybrid DC circuit breaker based on oscillation circuit. *J. Power Electron.* **2021**, *21*, 214–223. [CrossRef]
45. Zhang, Z.J.; Saeedifard, M. Overvoltage Suppression and Energy Balancing for Sequential Tripping of Hybrid DC Circuit Breakers. *IEEE Trans. Ind. Electron.* **2023**, *70*, 6506–6517. [CrossRef]
46. Mokhberdorani, A.; Carvalho, A.; Silva, N.; Leite, H.; Carrapatoso, A. Design and implementation of fast current releasing DC circuit breaker. *Electr. Power Syst. Res.* **2017**, *151*, 218–232. [CrossRef]
47. Li, C.; Liang, J.; Wang, S. Interlink Hybrid DC Circuit Breaker. *IEEE Trans. Ind. Electron.* **2018**, *65*, 8677–8686. [CrossRef]
48. Wang, D.; Liao, M.; Wang, R.; Li, T.; Qiu, J.; Li, J.; Duan, X.; Zou, J. Research on Vacuum Arc Commutation Characteristics of a Natural-Commutate Hybrid DC Circuit Breaker. *Energies* **2020**, *13*, 4823. [CrossRef]
49. Smith, M.W.; McCormik, M.D. *Transient Voltage Suppression Manual*, 3rd ed.; General Electric: Boston, MA, USA, 1982.
50. Zhang, Z.J.; Bosworth, M.; Xu, C.; Rockhill, A.; Zeller, P.; Saeedifard, M.; Graber, L.; Steurer, M. Lifetime-Based Selection Procedures for DC Circuit Breaker Varistors. *IEEE Trans. Power Electron.* **2022**, *37*, 13525–13537. [CrossRef]
51. Xu, C.; Rockhill, A.; Zhang, Z.J.; Bosworth, M.; Saeedifard, M.; Steurer, M.; Zeller, P.; Graber, L. Evaluation Tests of Metal Oxide Varistors for DC Circuit Breakers. *IEEE Open Acc. J. Power Energy* **2022**, *9*, 254–264. [CrossRef]

52. Rachi, M.R.K.; Husain, I. Main Breaker Switching Control and Design Optimization for A Progressively Switched Hybrid DC Circuit Breaker. In Proceedings of the 2020 IEEE Energy Conversion Congress and Exposition (ECCE), Detroit, MI, USA, 11–15 October 2020. [[CrossRef](#)]
53. Magnusson, J.; Saers, R.; Liljestrand, L.; Engdahl, G. Separation of the Energy Absorption and Overvoltage Protection in Solid-State Breakers by the Use of Parallel Varistors. *IEEE Trans. Power Electron.* **2014**, *29*, 2715–2722. [[CrossRef](#)]
54. Pang, T.; Manjrekar, M.D. A Surge Voltage Free Solid-State Circuit Breaker with Current Limiting Capability. In Proceedings of the IEEE Applied Power Electronics Conference and Exposition (APEC), Phoenix, AZ, USA, 14–17 June 2021. [[CrossRef](#)]
55. Gan, Z.; Yu, Z.; Nie, Z.; Qu, L.; Yan, X.; Huang, Y.; Zeng, R.; Gu, H. Coordinated DC Interruption Method Based on Magnetic Coupling Current-Limiting and Dissipation. *IEEE Trans. Power Electron.* **2023**, *38*, 2398–2407. [[CrossRef](#)]
56. Wu, T.; Wang, Z.; Fang, C.; Liu, S. Research on current limiting solid state circuit breaker for DC microgrid. *Electr. Power Syst. Res.* **2022**, *209*, 107950. [[CrossRef](#)]
57. Tracy, L.; Sekhar, P.K. Design and Testing of a Low Voltage Solid-State Circuit Breaker for a DC Distribution System. *Energies* **2020**, *13*, 338. [[CrossRef](#)]
58. Sen, S.; Mehraeen, S. Improving Low-Voltage DC Circuit Breaker Performance Through an Alternate Commutating Circuit. *IEEE Trans. Ind. Appl.* **2019**, *55*, 6127–6136. [[CrossRef](#)]
59. Kim, D.; Kim, S. Design and analysis of hybrid DC circuit breaker for LVDC grid systems. *J. Power Electron.* **2021**, *21*, 1395–1405. [[CrossRef](#)]
60. Rahimpour, S.; Husev, O.; Vinnikov, D. Design and Analysis of a DC Solid-State Circuit Breaker for Residential Energy Router Application. *Energies* **2022**, *15*, 9434. [[CrossRef](#)]
61. Li, W.; Wang, Y.; Wu, X.; Zhang, X. A Novel Solid-State Circuit Breaker for On-Board DC Microgrid System. *IEEE Trans. Ind. Electron.* **2019**, *66*, 5715–5723. [[CrossRef](#)]
62. Zhou, Z.Z.; Jiang, J.G.; Ye, S.; Liu, C.; Zhang, D. A Γ -source circuit breaker for DC microgrid protection. *IEEE Trans. Ind. Electron.* **2021**, *68*, 2310–2320. [[CrossRef](#)]
63. Diao, X.; Liu, F.; Song, Y.; Xu, M.; Zhuang, Y.; Zha, X. An Integral Fault Location Algorithm Based on a Modified T-Source Circuit Breaker for Flexible DC Distribution Networks. *IEEE Trans. Power Del.* **2021**, *36*, 2861–2871. [[CrossRef](#)]
64. Savaliya, S.G.; Fernandes, B.G. Analysis and experimental validation of bidirectional Z-source DC circuit breakers. *IEEE Trans. Ind. Electron.* **2020**, *67*, 4613–4622. [[CrossRef](#)]
65. Diao, X.; Liu, F.; Zhuang, Y.; Pan, S.; Zha, X. A Bidirectional Efficient Circuit Breaker with Automatic and Controllable Shutoff Functions for DC Distribution Network. *IEEE Trans. Ind. Electron.* **2023**, *70*, 7988–7999. [[CrossRef](#)]
66. Ryan, D.J.; Torresan, H.D.; Bahrani, B. A Bidirectional Series Z-Source Circuit Breaker. *IEEE Trans. Power Electron.* **2018**, *33*, 7609–7621. [[CrossRef](#)]
67. Ugalde-Loo, C.E.; Wang, Y.; Wang, S.; Ming, W.; Liang, J.; Li, W. Review on Z-Source Solid State Circuit Breakers for DC Distribution Networks. *CSEE J. Power Energy Syst.* **2023**, *9*, 15–27. [[CrossRef](#)]
68. Sun, Y.; Fan, Y.; Hou, J. Capacitor commutation type DC circuit breaker with fault character discrimination capability. *J. Power Electron.* **2023**, *23*, 1016–1027. [[CrossRef](#)]
69. Yu, Z.; Yan, X.; Zhang, X.; Qu, L.; Gan, Z.; Huang, Y. The Design and Development of a Novel 10 kV/60 kA Hybrid DC Circuit Breaker Based on Mixed Solid-State Switches. *IEEE Trans. Ind. Electron.* **2023**, *70*, 2440–2449. [[CrossRef](#)]
70. Qin, K.; Wang, S.; Ma, J.; Shu, J.; Zhang, R.; Liu, T. Thyristor-based DCCB with Reliable Fast Reclosing Protection Ability by Restoring Capacitor Polarity. *IEEE Trans. Power Electron.* **2023**, *38*, 7760–7770. [[CrossRef](#)]
71. Kheirollahi, R.; Zhao, S.; Lu, F. Fault Current Bypass-Based LVDC Solid-State Circuit Breakers. *IEEE Trans. Power Electron.* **2022**, *37*, 7–13. [[CrossRef](#)]
72. Shu, J.; Ma, J.; Wang, S.; Dong, Y.; Liu, T.; He, Z. A New Active Thyristor-Based DCCB With Reliable Opening Process. *IEEE Trans. Power Electron.* **2021**, *36*, 3617–3621. [[CrossRef](#)]
73. Marwaha, M.; Satpathi, K.; Sathik, M.H.M.; Pou, J.; Gajanayake, C.J.; Gupta, A.K.; Molligoda, D.; Surapaneni, R.K. SCR-Based Bidirectional Circuit Breaker for DC System Protection with Soft Reclosing Capability. *IEEE Trans. Ind. Electron.* **2023**, *70*, 4739–4750. [[CrossRef](#)]
74. Kheirollahi, R.; Zhao, S.; Zhang, H.; Lu, F. Fault Current Bypass-Based DC SSCB Using TIM-Pack Switch. *IEEE Trans. Ind. Electron.* **2023**, *70*, 4300–4304. [[CrossRef](#)]
75. Kheirollahi, R.; Zhao, S.; Zhang, H.; Lu, F. Fully Soft-Switched DC Solid-State Circuit Breakers. *IEEE Trans. Power Electron.* **2023**, *38*, 6750–6754. [[CrossRef](#)]

Disclaimer/Publisher’s Note: The statements, opinions and data contained in all publications are solely those of the individual author(s) and contributor(s) and not of MDPI and/or the editor(s). MDPI and/or the editor(s) disclaim responsibility for any injury to people or property resulting from any ideas, methods, instructions or products referred to in the content.